HHS Public Access

Author manuscript

Environ Pollut. Author manuscript; available in PMC 2023 January 17.

Published in final edited form as:

Environ Pollut. 2021 September 15; 285: 117411. doi:10.1016/j.envpol.2021.117411.

Assessing the Oxidative Potential of PAHs in Ambient $PM_{2.5}$ using the DTT Consumption Assay

Amber L. Kramer[1,2], **Shelby Dorn**[1], **Allison Perez**[2], **Courtney Roper**[3], **Ivan A. Titaley**[2], **Kaylee Cayton**[1], **Ronald P Cook**[4], **Paul H.-Y. Cheong**[1], **Staci L. Massey Simonich**[1,2]

[1]–Oregon State University Department of Chemistry, Lakewood Colorado

[2]–Oregon State University Department of Environmental and Molecular Toxicology, Lakewood Colorado

[3]–University of Mississippi Department of Biomolecular Sciences, Lakewood Colorado

[4]–Molecular Design Innovations, Lakewood Colorado

Abstract

The oxidative potential (OP) of atmospheric fine particulate matter ($PM_{2.5}$) has been linked to organic content, which includes polycyclic aromatic hydrocarbons (PAHs). The OP of 135 individual PAHs (including six subclasses) was measured using the dithiolthreitol (DTT) consumption assay. The DTT assay results were used to compute the concentration of each PAH needed to consume 50% of the DTT concentration in the assay (DTT_{50}), and the reduction potential of the PAHs (ΔG_{rxn}). Computed reduction potential results were found to match literature reduction potential values ($r^2 = 0.97$), while DTT_{50} results had no correlations with the computed ΔG_{rxn} values ($r^2 < 0.1$). The GINI equality index was used to assess the electron distribution across the surface of unreacted and reacted PAHs. GINI values correlated with ΔG_{rxn} in UPAH, HPAH, and OHPAH subclasses, as well as with all 135 PAHs in this study but did not correlate with DTT_{50}, indicating that electron dispersion is linked to thermodynamic reactions and structural differences in PAHs, but not linked to the OP of PAHs. Three ambient $PM_{2.5}$ filters extracts were measured in the DTT assay, alongside mixtures of analytical standards prepared to match PAH concentrations in the filter extracts to test if the OP follows an additive model of toxicity. The additive prediction model did not accurately predict the DTT consumption in the assay for any of the prepared standard mixtures or ambient $PM_{2.5}$ filter extracts, indicating a much more complex model of toxicity for the OP of PAHs in ambient $PM_{2.5}$. This study combined computed molecular properties with toxicologically relevant assay results to probe the OP of anthropogenically driven portions of ambient $PM_{2.5}$, and results in a better understanding of the complexity of ambient $PM_{2.5}$ OP.

*Corresponding Author Tel: (805) 794-0524. alkramer@g.ucla.edu.

6.0 ASSOCIATED CONTENT

6.1 Supporting Information

Tables S1-S2 provide additional information on the chemicals in this study, measured and calculated results. Tables S3-S4 provide correlation results. Figure S1 shows the DTT reactions occurring in the assay. Figure S2 shows structural characteristics used for correlation analysis with assay results. Table S5 provides ambient $PM_{2.5}$ filter and mixtures measurements in the DTT assay. Table S6 provides full computational results for GINI inequality values for compounds.

The authors declare no conflicts of interest.

Graphical Abstract

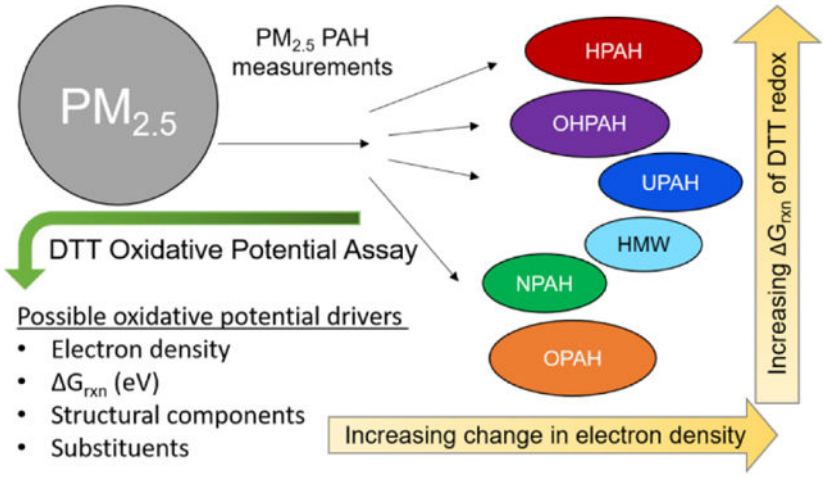

1 Introduction

Reactive oxygen species (ROS), created through exposure to fine particulate matter ($PM_{2.5}$), have been linked to inflammation, cardiopulmonary and respiratory diseases, and even cancer through various oxidative stress pathways [1 - 2]. $PM_{2.5}$ has been deemed by both the US Environmental Protection Agency (EPA) and the World Health Organization (WHO) as the most dangerous portion of atmospheric particulate matter (PM) to human health [3, 4]. Recent studies have indicated that the anthropogenically enhanced organic portion of $PM_{2.5}$ is directly linked to the oxidative potential of $PM_{2.5}$ [5 - 6]. The ability of a sample to cause cellular oxidative stress is referred to as oxidative potential (OP) and can be measured using various cellular and chemical assays and acellular assays [7 - 8, 9]. The dithiothreitol (DTT) assay uses a chemical redox reaction to determine the amount of ROS produced, and has been increasing in use for evaluating the OP of the organic portions of atmospheric PM due to demonstrated correlation with biological OP assays [10, 11]. Classes of compounds found in $PM_{2.5}$, such as polycyclic aromatic hydrocarbons (PAHs), have been linked to oxidative stress through cellular assays [12, 13]. The elucidation of the OP of components of $PM_{2.5}$, such as individual PAHs, could improve predictive modeling of $PM_{2.5}$ OP, and is a growing area of research, particularly using the DTT assay [14]. Finding a predictive model for OP of $PM_{2.5}$ would aid the assessment of human health impacts of $PM_{2.5}$ exposures [13, 15, 16, 17, 14].

PAHs are a class of compounds emitted through incomplete combustion which undergo long-range atmospheric transport entrapped in $PM_{2.5}$ [18, 19]. Unsubstituted PAHs (UPAHs) are directly emitted through combustion processes. Sixteen UPAHs appear on the US EPA Priority Pollutant List (PPL) due to their characterized toxicity, and availability of standards at the time the list was made [20, 21]. Other subclasses of PAHs have since been measured in atmospheric $PM_{2.5}$ samples along with UPAHs, but there is limited data on their toxicity, or individual oxidative potentials [19, 22 - 23]. These substituted PAHs can be directly emitted from combustion sources along with UPAHs, such as heterocyclic PAHs (HPAHs), which contain a non-carbon atom in the ring-structures, oxy PAHs (OPAHs) which contain a carbonyl oxygen substituted outside the rings, and have been linked to oxidative stress

in humans, and high molecular weight (HMW) PAHs, which are less volatile and have a molecular mass over 300 AMU [22, 24, 25]. UPAHs can also undergo atmospheric reactions leading to nitro (NPAHs) and hydroxy (OHPAHs) substitutions on the UPAH rings [24, 26]. While many studies have looked at the carcinogenic, mutagenic, and developmental toxicity of individual PAHs, the OP of individual PAHs measured in ambient $PM_{2.5}$ has not been evaluated using the DTT consumption assay [24, 27, 28, 22, 14].

For the first time, we combined the use of the DTT consumption assay to evaluate the OP of 135 individual PAHs (23 UPAHs, 24 NPAHs, 18 OPAHs, 12 HPAHs, 15 HMWs and 43 OHPAHs), with computational chemical models to attempt to predict the OP of PAHs in ambient $PM_{2.5}$ filter extracts, along with mixtures of PAH standards prepared to match measured $PM_{2.5}$ PAH concentrations. We calculated a DTT_{50}, (the concentration of each compound required to consume 50% of the DTT in the assay), as a representation of the OP, and to allow comparison of this OP between individual PAHs as well as the subclasses of PAHs. To assess if currently available computational modeling could predict the PAH OP in $PM_{2.5}$, the DTT consumption assay results were used to calculate the Gibbs free energy (ΔG_{rxn}) of the redox reaction, and also compared to various structural components of PAHs, as well as electron density across each PAH using the GINI (statistical measurement of unevenness) method [29, 30]. By combining computational analysis with assay analysis, we demonstrate the efficacy of the DTT consumption assay to reliably predict the reduction potentials of PAHs. We also demonstrate the complexity of the OP in mixtures, as well as in ambient $PM_{2.5}$, and the inability, thus far, to model OP using DTT consumption results alone.

2 Materials and Methods

2.1 Materials.

Compound names, CAS numbers, molecular mass, abbreviations, and sources in $PM_{2.5}$, can be found on Table S1 of the Supplemental Information. Analytical standards were dissolved in dimethylsulfoxide (DMSO) and diluted to ~1 mM concentration. For individual DTT consumption assay analysis, six-point concentration ranges for each PAH were made by diluting standards dissolved in DMSO to between 20–100 μM in DMSO. Concentration ranges were measured in triplicate, along with controls of non-reacted PAH of the same six concentration points. Linear results of PAH concentration and DTT consumption were calculated and used to calculate the concentration of each PAH required to use up to 50% of the DTT (DTT_{50}), allowing for comparisons between individual PAH results in terms of the DTT_{50}, as a measure of OP.

2.2 DTT assay.

DTT assay reaction can be found in Figures S1. DTT was dissolved in 0.05 M monobasic potassium phosphate buffer (PBS), making a 5 mM solution of DTT. As described elsewhere, six-point calibration curves of DTT were made by diluting the stock solution to between 0 and 1 mM concentrations [31 32]. For sample exposure, DTT stock was diluted to 1 mM, and 5 μL were added to samples in each well. DTNB (5,5-dithio-bis-2-nitrobenzoic

acid) was dissolved in methanol to a concentration of 10 mM. For reaction quenching, DTNB was diluted to 1 mM in PBS and 10 μL wase added to wells[31 32].

DTT consumption assay was performed in flat bottom 96 well plates. Wells were first prepared with 100 μL of 5.0 mM PBS buffer, then, for DTT calibration curves, 10 μL of DMSO and 5 μL of DTT calibration standard was added [33]. Sample wells were prepared by adding 10 μL of each PAH concentration, (or analyte mixture or extract), to the PBS buffer. Lastly, 5 μL of 1 mM DTT was added to the sample wells, and plates were incubated at 37°C for 15 minutes. Control wells were volume corrected by supplementing additional 5.0 mM PBS buffer to ensure all wells had a final volume of 125 μL. After incubation, 10 μL of 1 mM DTNB was added to all wells to quench DTT reactions, and plates were gently shaken for 5 minutes. Absorbance (412 nm) was measured using a BioTek Synergy HTX multimode reader (Winooski, Vermont, USA).

2.3 Computations.

The Gibbs free energy (ΔG_{rxn}) of the redox reaction involving PAHs and DTT (Figure S1) was calculated for both the parent PAH as well as the radical anion PAH, based on equation 1 and the calculated DTT_{50} of each PAH. Geometry optimizations were performed using density functional theory (DFT) B3LYP [34] with the 6–311++G(d,p) [35 - 36] basis set in Gaussian 09 [37]. All geometry optimizations and thermal corrections were performed in the gas phase at 298 K. Refined single-point energies were computed in ORCA at the DLPNO-CCSD(T)/def2-TZVPP level of theory [38 - 39]. Both steps were performed for all molecules involved in the reaction (equation 1). The computed ΔG_{rxn} of PAHs was compared to available literature reduction potential values and with the DTT_{50} [40, 41].

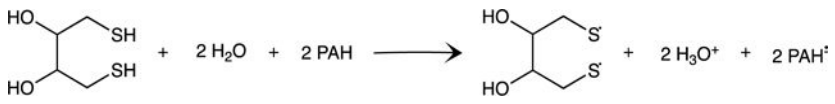

Equation 1:

Structural composition was considered for possible differences in ΔG_{rxn} observed between isomers. Understanding that PAH structural components such as a bay region containing only 6-atom rings, versus bay regions that have at least one 5-atom ring involved in the bay would have differences in electron density (Figure S2), the numbers of these features were summed for each molecule and used for correlation analysis (Table S4). The structural components considered are illustrated in Figure S2 and are combined in the main correlation data as “Structural Component” (Table S2).

2.4 GINI Value Methods.

To assess if the OP of each PAH was related to the electron density throughout each molecule, GINI index values for inequality were calculated for each PAH [29 30, 42]. The GINI index is a statistical measure of the unevenness of a population. In Baders’ Quantum Theory of Atoms in Molecules,[47] the electron densities of a molecule can be partitioned into atom basins and further partitioned into unshared, shared-bonded, and shared-nonbonded

pair densities. The GINI indices of these electron densities are related to the concepts of chemical hardness and charge transfer capacity and has been shown to be a reliable predictive tool for pK_as of substituted aromatic carboxylic acids and the aromaticity of multi-ring aromatics[40, 41].

The optimized parent (P) molecule and resulting radical anion (A) PAH structures were analyzed with AIMAll software package (Table S6) [43, 44]. A localization / delocalization matrix was extracted for both states (P and A) of each PAH and used to calculate two GINI index values for potential indicators of OP. The first GINI index value calculated was for the equity of electron density at localized non-hydrogen atoms, while the second GINI index value was calculated for the equity of electron localization / delocalization on and between bonded (non-hydrogen) atoms. GINI index values range between 0 and 1, with 0 representing total equality for electron density across the potential indicator (for example the electron density of the carbon atoms in benzene equals 1), and 1 representing total inequality [29]. The change in electron density across the molecules for both the localized GINI values and the GINI values calculated for all electrons during reduction was calculated by subtracting the anionic GINI (A_{GINI}) values from the parent molecule GINI (P_{GINI}) values (P_{GINI} - A_{GINI}).

2.5 Structural analysis.

Several structural features of PAHs were used to analyze for correlations with the DTT results. Several isomers of PAHs were found to have different results in the DTT assay. For instance Phenanthrene, a three ringed bent PAH resulted in a DTT_{50} concentration of 72 μM, while the three ringed straight isomer, Anthracene, resulted in a DTT_{50} concentration of 17 μM (Table S2). To assess if the structural conformation of such isomers was responsible for the differences in OP results, a number of structural characteristics (Figure S2) were summed up for each of the 135 PAHs and used for correlation analysis.

2.6 $PM_{2.5}$ samples.

Three available ambient $PM_{2.5}$ samples were each collected using a Tisch Environmental (Village of Cleves Ohio, USA) high volume cascade impactor on quartz fiber filters (QFF) for a 24 hour period along the northern coast of the US State of Washington during the spring of 2018 [23]. The $PM_{2.5}$ samples were collected alongside samples for another study, with detailed filter handling, extraction and quantification processes are detailed elsewhere [23], in short, filters were stored at −20°C until undergoing extraction via accelerated solvent extraction (ThermoFisher (USA) Dionex ASE 350). Filter extractions underwent a cleanup step using solid phase extraction, and concentration, under a fine nitrogen stream, before aliquoting portions for quantitative analysis. PAH analysis of each of the extracts was performed using gas chromatography mass spectrometry (GC/MS) operated in electron Impact mode (UPAH, HPAH, OPAH, OHPAH (Agilent 7890), and HMW (Agilent 6890N) analysis) and in negative chemical ionization (NPAH (Agilent 6890) analysis) using established quantitative methods with UPAH = 81%, HMW = 86%, NPAH = 124%, OPAH = 127%, HPAH = 76%, and OHPAH 54% recovery rates for each class [24, 45, 23]. DTT analysis of the $PM_{2.5}$ extracts followed the same steps as the individual PAH standards. $PM_{2.5}$ filter extracts were stored at 4°C. An aliquot of 100 μL of the extract from each of

the three ambient $PM_{2.5}$ filters was evaporated to near dryness under fine nitrogen stream. To help reduce evaporation loss of volatile PAHs from extracts, the vials of aliquots were incased in ice during concentration. Before total dryness was observed, 100 μL of DMSO was added to the aliquots and evaporation continued for ~10 minutes to ensure solvent evaporation. From this stock solution, dilutions were made for final total PAH concentration of 1.5 mM (± 0.3) for use in the DTT assay. For analysis 10 μL of each filter extract was used in the DTT assay. Each of the three filters (A, B, and C) were analyzed in six separate wells to ensure statistical viability.

To assess if the total DTT consumption could be predicted by the measured individual PAH DTT consumption rates, mixtures of US EPA Priority Pollutant List (PPL) PAHs standards (*PPL*), and mixtures of standards of the entire suite of measured PAHs (*Whole*) were prepared in DMSO to match measured concentrations of PAHs for the three (A, B, C) ambient $PM_{2.5}$ filter extracts (*Extracts*). Measured PAH concentrations for the Extracts can be found in Table S2. The Whole and PPL mixtures were measured alongside Extracts the in the DTT consumption assay for a total concentration (based on chemical composition) of 35 – 59 μM. *Extracts*, *PPL* mixtures, and *Whole* mixtures were measured in replicates of six in the DTT consumption assay, with the consumed concentration (mM) of DTT reported as average (± 1 Standard Error) in Table S5.

2.7 Statistical analysis.

Statistical analysis was performed using R statistical software on the RStudio user platform (v 3.6.2). Pearson's Correlations were performed to assess if given parameters were related to each other, which may be linked to the OP of the molecules. Student's t-tests were performed to establish differences or similarities between data sets. One-way ANOVA on ranks was performed using the Dunn's Method applied to the Kruskal-Wallis test. All reported statistical significance is based on p-value ≤ 0.05.

3 Results

3.1 DTT assay results.

DTT_{50} concentrations (the concentration of each PAH required to use up 50% of the DTT in the assay) were not strongly correlated with the calculated molecular properties (reduction potentials, and changes in electron density) in this study (Table 1). DTT_{50} was statistically negatively correlated to molecular mass of all 135 PAHs, but was not correlated to any of the other parameters identified in this study. (Tables 1, Table S3). Within each class of PAH only the number of OH substitutions on OHPAHs had correlation with the measured DTT_{50} concentrations (Table S3).

Comparisons of DTT_{50} concentrations per PAH class and the computed ΔG_{rxn} for each class showed that there was no statistically significant difference between the average DTT_{50} of each PAH class (Figure 1). Applying the Dunn's Method to account for different numbers of PAHs in each class allowed for a Kruska-Wallis one-way ANOVA on ranks analysis and resulted in significantly lower ΔG_{rxn} of OPAH and NPAH from UPAHs, HPAHs, and OHPAHs (Figure 1). Figure 1 also shows the relative abundance of each class of

PAH measured in 96 ambient $PM_{2.5}$ samples collected between 2016 and 2018 along the northwest coast of the state of Washington for a previous study by this group [23].

3.2 Computational analysis.

The calculated ΔG_{rxn} of all PAHs were found to have a number of correlations with other parameters in this study, as well within different subclasses of PAHs (Table 1). The ΔG_{rxn} was statistically correlated with the molecular mass (AMU) of all 135 PAHs used in this study (ALL), as well as with UPAH, NPAH and OHPAH classes. The change (Parent – Anionic) in both localized electron density and all electron density (delocalized) across the molecule were correlated with the ΔG_{rxn} for all 135 PAHs, as well as the UPAH, NPAH, and OHPAH classes of PAHs. Localized electron density changes were correlated with the type and number of substituents, where only NPAHs had correlations between all electron density and the number of substituents (Tables 1). There were correlations of both ΔG_{rxn} and GINI values with structural bay regions of different ring proportions in UPAHs (Figure S2 & Table S3).

To assess if the reduction potential calculated from the DTT assay was accurate, available documented reduction potential (eV) of several PAHs was compared to the ΔG_{rxn} from this study (Figure 2) [40, 41]. The strong correlation ($r^2 = 0.97$) of the documented reduction potential with the calculated ΔG_{rxn} (Figure 2), demonstrated the accuracy of the DTT assay to measure the reduction of individual PAHs. However, when attempting to use the ΔG_{rxn} values to predict DTT_{50}, there was no correlation ($r^2 < 0.1$) for these individual PAHs (Figure 2).

3.3 Ambient $PM_{2.5}$ filter and PAH Mixture Results.

PAH concentrations measured in the DTT assay were used to create linear regression models for each PAH. Using these regressions, and the measured concentration of each PAH found in ambient $PM_{2.5}$ filter extracts, the consumption of DTT for mixtures and extracts was calculated assuming an additive OP model (Table 1). If OP followed the additive model, the predicted DTT consumption would match the DTT assay results. Figure 3 shows the measured DTT assay results for the three ambient $PM_{2.5}$ filter extracts, along with mixtures of analytical standards made to match the concentrations of PAHs measured in the extracts. The calculated DTT consumption concentrations were plotted (triangles) against the measured DTT consumption (bars) of extracts and mixtures of PAH standards to determine if the OP were additive (Figure 3). Extract measurements were significantly different from Whole PAH standard mixture measurements (Filters A and B), or the mixtures of the 16 PAHs on the EPA priority pollutant list (PPL) measurements (Filter C) (Figure 3, Table S4).

4.0 Discussion

Based on equation 1, a lower ΔG_{rxn} value indicates a more favorable oxidation of DTT by a given PAH and, therefore, a greater OP. Results shown in Figure 1 indicate that OPAH and NPAH have a greater OP than UPAHs, HPAHs, and OHPAHs, based on the statistically different average ΔG_{rxn} per class. Previous studies have linked OP to quinones[46 47], of which

there were fourteen in the measured OPAHs in this study (Table S1). The lack of statistically significant differences in DTT_{50} between classes of PAHs (Figure 1) indicates that the OP of individual PAHs, or classes of PAHs, is a more complex phenomenon than was captured by ΔG_{rxn} measured in the DTT assay. While molecular mass for all 135 tested PAHs was correlated with DTT_{50}, the substitution of PAHs was not a significant predictor of OP in the DTT consumption assay.

Individual PAH comparisons of computed ΔG_{rxn} from the DTT results with available documented reduction potentials of individual PAHs [40, 41], as shown in Figure 2, suggest that the PAH-DTT reaction follows thermodynamic principles measured through more typical electrochemical experimentation. However, the lack of correlation between measured DTT_{50} concentrations and ΔG_{rxn} values ($R^2 = 0.04$), indicate that thermodynamic properties alone, do not explain the OP of the PAHs measured in this study (Figure 2). The lack of correlation between the DTT consumption, (as a representation of the OP), and the thermodynamic properties calculated here, is further supported by the inability of the DTT assay results to predict the OP of the PAHs in $PM_{2.5.}$ The lack of the additive model of DTT consumption to predict measured OP of mixtures of PAHs and extracts of ambient $PM_{2.5}$ in this study support previous studies that have demonstrated synergistic, additive, and antagonistic effects of quinones [46, 47], 14 of which were included in the OPAH compounds in this study (Table S1). Beyond the quinones, the 121 other PAHs may also be enhancing the suggested synergistic, additive, and/or antagonistic effects of the components of $PM_{2.5}$ on overall OP.

The use of the GINI inequality system allowed us to examine what effect the reduction of each PAH had on the electron dispersion across the surface of each molecule. While no correlation was found between DTT_{50} and of the computed GINI values in this study, there were correlations between structural components and substituents with the change in electron dispersion (GINI values analysis) when PAHs underwent the redox reaction in the DTT assay (Tables S2 and S3). This illustrates how electron affinity between different incorporated non-carbon atoms (sulfur, nitrogen, and/or oxygen) can change the OP of a molecule. Structural correlations (Table S3) within HMW and UPAH subclasses can help to explain differences between isomers of the same molecular mass. Figure 4 shows the difference between GINI values for parent and anionic PAH classes for localized electrons (red and blue boxes), as well as the GINI values when all electrons were used in the calculations (green and orange). Statistical analysis shows that the difference in electron dispersion between the parent PAHs and the radical anions produced in the redox reaction are significant for UPAH, OPAH, NPAH and OHPAHs, in both forms of electron calculations.

Analysis of the computed GINI values (Table S5) indicates that the re-dox reduction of PAHs, either localized electrons only, or both local and delocalized electrons, results in more equity in the distribution of electrons across the surface of the PAH molecules (Figure 4). While the results of this work do not indicate that the GINI values can be used in modeling OP, the demonstration of PAHs to accommodate an additional electron (reduction) provide insight into the thermodynamics of PAHs, suggesting a longer lifetime of these radical anions that previously assumed. The statistical correlations of GINI values with

ΔG_{rxn} values (Tables 1 & S3) in all of the 135 PAHs, as well as with the UPAH, NPAH, and OHPAH classes, indicate that the electron distribution across the surface of PAHs could be useful in the determination of PAH toxicity.

The ambient $PM_{2.5}$ filter results, shown in Figure 3, demonstrate the complexity of OP in ambient $PM_{2.5.}$ These limited results support other works that have suggested additional factors, such as antagonistic effects, that need to be assessed to fully be able to model OP from $PM_{2.5}$ chemical characterization studies [47]. Measuring only the PPL PAHs resulted in the underrepresentation of the ROS generating components of $PM_{2.5}$ in this limited ambient sampling. While it has been suggested that PAHs provide a synergistic effect on OP of $PM_{2.5}$ [13], these results suggest the OP of PAHs likely follows a non-additive or antagonistic model (Table S4).

5.0 Conclusions

The results of this study illustrate that, while the DTT assay has documented similarity to biological assays for measuring oxidative stress [10, 11], the DTT assay results, in terms of the measured DTT_{50}, do not correlate with thermodynamically driven molecular properties commonly used for computational modeling of the individual PAHs in this study. While several computational parameters assessed here correlate with each other, demonstrating the efficacy of the DTT assay to measure the reduction potential of PAHs, the lack of correlation between DTT_{50} results and any of the computed parameters demonstrates the continued need to further assess $PM_{2.5}$ components, their interactions, and the complex nature of the OP of PAHs in $PM_{2.5}$. Examination of the three ambient $PM_{2.5}$ filters used in this study, illustrate that, while only PPL PAHs are measured in most $PM_{2.5}$ screenings [21], they do not account for all of the OP of the $PM_{2.5}$ extracts (Figure 3 and Table S4). The largest overall concentration percent of measured PAHs was HPAHs in each of the analyzed $PM_{2.5}$ filters (Table S2) while OPAHs (second largest overall percent composition of PAHs in $PM_{2.5}$) had the lowest ΔG_{rxn}. The measurement of substituted PAHs in ambient $PM_{2.5}$, along with the OP of these compounds measured in this study, adds to the growing evidence for the expansion of air monitoring campaigns to quantify PAH compounds not included on the USEPA's PPL [21]. Further exploration of the drivers of OP in ambient $PM_{2.5}$ should include synergistic and antagonistic drivers of OP, such as ionic salts, metals, and non-volatile organic compounds, as well as physical characteristics such as the metal-organic framework and surface functionalities of the particles themselves, which have been shown in other works to effect the production of ROS [48, 49]. The ability to fully model the potential OP of ambient $PM_{2.5}$ in order to protect communities from harmful exposure events, will no doubt require more interdisciplinary research into the physical and chemical nature of atmospheric PM. Future studies should include ambient PM collected in different atmospheric environments, to better understand the if the OP of $PM_{2.5}$ is universal, or if specific regional atmospheric conditions might change the OP of $PM_{2.5}$ exposure.

Supplementary Material

Refer to Web version on PubMed Central for supplementary material.

ACKNOWLEDGEMENTS

This publication was made possible in part by Grant Numbers AGS-1411214 from the National Science Foundation (NSF), and P42-ES016465 and P30-ES00210, from National Institute of Environmental Health Sciences (NIEHS), National Institute of Health (NIH). Its contents are the sole responsibility of the authors and do not represent the official view of the NIEHS or NIH.

10.0 REFERENCES

1. Thurston GD; Kipen H; Annesi-Maesano I; Balmes J; Brook RD; Cromar K; De Matteis S; Forastiere F; Forsberg B; Frampton MW; Grigg J; Heederik D; Kelly FJ; Kuenzli N; Laumbach R; Peters A; Rajagopalan ST; Rich D; Ritz B; Samet JM; Sandstrom T; Sigsgaard T; Sunyer J; Brunekreef B, A joint ERS/ATS policy statement: what constitutes an adverse health effect of air pollution? An analytical framework. European Respiratory Journal 2017, 49 (1), 1600419.
2. Crobeddu B; Baudrimont I; Deweirdt J; Sciare J; Badel A; Camproux A-C; Bui LC; Baeza-Squiban A, Lung Antioxidant Depletion: A Predictive Indicator of Cellular Stress Induced by Ambient Fine Particles. Environmental Science & Technology 2020.
3. Agency, E. P. Particulate Matter (PM) Basics. https://www.epa.gov/pm-pollution/particulate-matter-pm-basics (accessed 1 April 2021).
4. Organization, W. H. Ambient (outdoor) air pollution. https://www.who.int/news-room/fact-sheets/detail/ambient-(outdoor)-air-quality-and-health (accessed 1 April 2021).
5. Athanasios Valavanidis TV, Konstantinos Fiotakis, Spyrdion Loridas, Pulmonary Oxidative Stress, Inflammation and Cancer: Respirable Particulate Matter, Fibrous Dust and Ozone as Major Causes of Lung Carcinogenisis through Reactive Oxygen Species Mechanisms. International Journal of Environmental Research and Public Health 2013, 10 (9), 3886–3907. [PubMed: 23985773]
6. Tuet WY; Chen Y; Xu L; Fok S; Gao D; Weber RJ; Ng NL, Chemical oxidative potential of secondary organic aerosol (SOA) generated from the photooxidation of biogenic and anthropogenic volatile organic compounds. Atmos. Chem. Phys. 2017, 17 (2), 839–853.
7. Abrams JY; Weber RJ; Klein M; Samat SE; Chang HH; Strickland MJ; Verma V; Fang T; Bates JT; Mulholland JA; Russell AG; Tolbert PE, Associations between Ambient Fine Particulate Oxidative Potential and Cardiorespiratory Emergency Department Visits. Environ Health Persp 2017, 125 (10), 107008–107008.
8. Lin Y-H; Arashiro M; Martin E; Chen Y; Zhang Z; Sexton KG; Gold A; Jaspers I; Fry RC; Surratt JD, Isoprene-Derived Secondary Organic Aerosol Induces the Expression of Oxidative Stress Response Genes in Human Lung Cells. Environmental Science & Technology Letters 2016, 3 (6), 250–254.
9. Feng Y; Kleinstreuer C; Rostami A, Evaporation and condensation of multicomponent electronic cigarette droplets and conventional cigarette smoke particles in an idealized G3–G6 triple bifurcating unit. Journal of Aerosol Science 2015, 80, 58–74.
10. Ayres JG; Borm P; Cassee FR; Castranova V; Donaldson K; Ghio A; Harrison RM; Hider R; Kelly F; Kooter IM; Marano F; Maynard RL; Mudway I; Nel A; Sioutas C; Smith S; Baeza-Squiban A; Cho A; Duggan S; Froines J, Evaluating the Toxicity of Airborne Particulate Matter and Nanoparticles by Measuring Oxidative Stress Potential—A Workshop Report and Consensus Statement. Inhalation Toxicology 2008, 20 (1), 75–99. [PubMed: 18236225]
11. Tong H; Lakey PSJ; Arangio AM; Socorro J; Shen F; Lucas K; Brune WH; Pöschl U; Shiraiwa M, Reactive Oxygen Species Formed by Secondary Organic Aerosols in Water and Surrogate Lung Fluid. Environmental Science & Technology 2018, 52 (20), 11642–11651. [PubMed: 30234977]
12. Bortey-Sam N; Ikenaka Y; Akoto O; Nakayama SMM; Asante KA; Baidoo E; Obirikorang C; Saengtienchai A; Isoda N; Nimako C; Mizukawa H; Ishizuka M, Oxidative stress and respiratory symptoms due to human exposure to polycyclic aromatic hydrocarbons (PAHs) in Kumasi, Ghana. Environmental Pollution 2017, 228, 311–320. [PubMed: 28551561]
13. Bae S; Pan XC; Kim SY; Park K; Kim YH; Kim H; Hong YC, Exposures to Particulate Matter and Polycyclic Aromatic Hydrocarbons and Oxidative Stress in Schoolchildren. Environ Health Persp 2010, 118 (4), 579–583.

14. Bates JT; Fang T; Verma V; Zeng L; Weber RJ; Tolbert PE; Abrams J; Sarnat SE; Klein M; Mulholland JA; Russell AG, Review of acellular assays of ambient particulate matter oxidative potential: methods and relationships with composition, sources, and health effects. Environmental Science & Technology 2019.
15. Lu S.-y.; Li Y.-x.; Zhang J.-q.; Zhang T; Liu G.-h.; Huang M.-z.; Li X; Ruan J.-j.; Kannan K; Qiu R.-l., Associations between polycyclic aromatic hydrocarbon (PAH) exposure and oxidative stress in people living near e-waste recycling facilities in China. Environment International 2016, 94, 161–169. [PubMed: 27258657]
16. Liu H-H; Lin M-H; Chan C-I; Chen H-L, Oxidative damage in foundry workers occupationally co-exposed to PAHs and metals. International Journal of Hygiene and Environmental Health 2010, 213 (2), 93–98. [PubMed: 20153695]
17. Kaur M; Raval K; Flores D; Olivas M; Waterston A; Hasson A; Dejean L, Understanding PM2.5-Induced Oxidative Stress In Alveolar Macrophages. The FASEB Journal 2020, 34 (S1), 1–1.
18. Primbs T; Piekarz A; Wilson G; Schmedding D; Higginbotham C; Field J; Simonich SM, Influence of Asian and Western United States Urban Areas and Fires on the Atmospheric Transport of Polycyclic Aromatic Hydrocarbons, Polychlorinated Biphenyls, and Fluorotelomer Alcohols in the Western United States. Environmental Science & Technology 2008, 42 (17), 6385–6391. [PubMed: 18800505]
19. Genualdi SA; Killin RK; Woods J; Wilson G; Schmedding D; Simonich SLM, Trans-Pacific and Regional Atmospheric Transport of Polycyclic Aromatic Hydrocarbons and Pesticides in Biomass Burning Emissions to Western North America. Environmental Science & Technology 2009, 43 (4), 1061–1066. [PubMed: 19320158]
20. Agency, U. S. E. P., Priority Pollutant List. 2014.
21. Andersson JT; Achten C, Time to Say Goodbye to the 16 EPA PAHs? Toward an Up-to-Date Use of PACs for Environmental Purposes. Polycyclic Aromatic Compounds 2015, 35 (2–4), 330–354. [PubMed: 26823645]
22. Wang W; Jariyasopit N; Schrlau J; Jia Y; Tao S; Yu T-W; Dashwood RH; Zhang W; Wang X; Simonich SLM, Concentration and Photochemistry of PAHs, NPAHs, and OPAHs and Toxicity of PM2.5 during the Beijing Olympic Games. Environmental Science & Technology 2011, 45 (16), 6887–6895. [PubMed: 21766847]
23. Kramer AL; Campbell L; Donatuto J; Heidt M; Kile M; Massey Simonich SL, Impact of local and regional sources of PAHs on tribal reservation air quality in the U.S. Pacific Northwest. Science of The Total Environment 2020, 710, 136412.
24. Jariyasopit N; McIntosh M; Zimmermann K; Arey J; Atkinson R; Cheong PH-Y; Carter RG; Yu T-W; Dashwood RH; Massey Simonich SL, Novel Nitro-PAH Formation from Heterogeneous Reactions of PAHs with NO2, NO3/N2O5, and OH Radicals: Prediction, Laboratory Studies, and Mutagenicity. Environmental Science & Technology 2014, 48 (1), 412–419. [PubMed: 24350894]
25. Zhao Y; Hong B; Fan Y; Wen M; Han X, Accurate analysis of polycyclic aromatic hydrocarbons (PAHs) and alkylated PAHs homologs in crude oil for improving the gas chromatography/mass spectrometry performance. Ecotoxicology and Environmental Safety 2014, 100 (Supplement C), 242–250. [PubMed: 24229786]
26. Kramer AL; Suski KJ; Bell DM; Zelenyuk A; Massey Simonich SL, Formation of Polycyclic Aromatic Hydrocarbon Oxidation Products in α-Pinene Secondary Organic Aerosol Particles Formed through Ozonolysis. Environmental Science & Technology 2019, 53 (12), 6669–6677. [PubMed: 31125204]
27. Geier MC; Chlebowski AC; Truong L; Massey Simonich SL; Anderson KA; Tanguay RL, Comparative developmental toxicity of a comprehensive suite of polycyclic aromatic hydrocarbons. Arch Toxicol 2018, 92 (2), 571–586. [PubMed: 29094189]
28. Trine LSD; Davis EL; Roper C; Truong L; Tanguay RL; Simonich SLM, Formation of PAH Derivatives and Increased Developmental Toxicity during Steam Enhanced Extraction Remediation of Creosote Contaminated Superfund Soil. Environmental Science & Technology 2019, 53 (8), 4460–4469. [PubMed: 30957485]
29. Lerman R; Yitzhaki S, A note on the calculation and interpretation of the Gini index. Economics Letters 1984, 15 (3–4), 363–368.

30. Jiang L; Chen H; Pinello L; Yuan G-C, GiniClust: detecting rare cell types from single-cell gene expression data with Gini index. Genome Biology 2016, 17 (1), 144. [PubMed: 27368803]

31. Patel A; Rastogi N, Oxidative potential of ambient fine aerosol over a semi-urban site in the Indo-Gangetic Plain. Atmospheric Environment 2018, 175, 127–134.

32. Kramer AJ; Rattanavaraha W; Zhang Z; Gold A; Surratt JD; Lin Y-H, Assessing the oxidative potential of isoprene-derived epoxides and secondary organic aerosol. Atmospheric Environment 2016, 130, 211–218.

33. Roper C; Perez A; Barrett D; Hystad P; Massey Simonich SL; Tanguay RL, Workflow for comparison of chemical and biological metrics of filter collected PM2.5. Atmospheric Environment 2020, 117379.

34. Becke AD, Density-functional thermochemistry. III. The role of exact exchange. The Journal of Chemical Physics 1993, 98 (7), 5648–5652.

35. McLean AD; Chandler GS, Contracted Gaussian basis sets for molecular calculations. I. Second row atoms, Z=11–18. The Journal of Chemical Physics 1980, 72 (10), 5639–5648.

36. Frisch MJ; Pople JA; Binkley JS, Self-consistent molecular orbital methods 25. Supplementary functions for Gaussian basis sets. The Journal of Chemical Physics 1984, 80 (7), 3265–3269.

37. Frisch MJ, G. W. T., Schlegel HB, Scuseria GE, Robb MA, Cheeseman JR, Scalmani G, Barone V, Petersson GA, Nakatsuji H, Li X, Caricato M, Marenich A, Bloino J, Janesko BG, Gomperts R, Mennucci B, Hratchian HP, Ortiz JV, Izmaylov AF, Sonnenberg JL, Williams-Young D, Ding F, Lipparini F, Egidi F, Goings J, Peng B, Petrone A, Henderson T, Ranasinghe D, Zakrzewski VG, Gao J, Rega N, Zheng G, Liang W, Hada M, Ehara M, Toyota K, Fukuda R, Hasegawa J, Ishida M, Nakajima T, Honda Y, Kitao O, Nakai H, Vreven T, Throssell K, Montgomery JA Jr., Peralta JE, Ogliaro F, Bearpark M, Heyd JJ, Brothers E, Kudin KN, Staroverov VN, Keith T, Kobayashi R, Normand J, Raghavachari K, Rendell A, Burant JC, Iyengar SS, Tomasi J, Cossi M, Millam JM, Klene M, Adamo C, Cammi R, Ochterski JW, Martin RL, Morokuma K, Farkas O, Foresman JB, and Fox DJ Gaussian 09, Gaussian, Inc: Wallingford, CT, USA, 2016.

38. Neese F, The ORCA program system. Wiley Interdisciplinary Reviews: Computational Molecular Science 2012, 2 (1), 73–78.

39. Weigend F, Accurate Coulomb-fitting basis sets for H to Rn. Physical Chemistry Chemical Physics 2006, 8 (9), 1057–1065. [PubMed: 16633586]

40. Modelli A; Mussoni L, Rapid quantitative prediction of ionization energies and electron affinities of polycyclic aromatic hydrocarbons. Chemical Physics 2007, 332 (2), 367–374.

41. Davis AP; Fry AJ, Experimental and Computed Absolute Redox Potentials of Polycyclic Aromatic Hydrocarbons are Highly Linearly Correlated Over a Wide Range of Structures and Potentials. The Journal of Physical Chemistry A 2010, 114 (46), 12299–12304. [PubMed: 21028773]

42. Lerman R; Yitzhaki S, Improving the accuracy of estimates of Gini coefficients. Journal of Econometrics 1989, 42 (1), 43–47.

43. Keith TA AIMAII, 19.10.12; TK Gristmill Software: Overland Park KS, USA, 2019.

44. Bader RFW, Atoms in Molecules - A Quantum Theory. Oxford University Press: Oxford UK, 1990.

45. Chibwe L; Geier MC; Nakamura J; Tanguay RL; Aitken MD; Simonich SLM, Aerobic Bioremediation of PAH Contaminated Soil Results in Increased Genotoxicity and Developmental Toxicity. Environmental Science & Technology 2015, 49 (23), 13889–13898. [PubMed: 26200254]

46. Lyu Y; Guo H; Cheng T; Li X, Particle Size Distributions of Oxidative Potential of Lung-Deposited Particles: Assessing Contributions from Quinones and Water-Soluble Metals. Environmental Science & Technology 2018, 52 (11), 6592–6600. [PubMed: 29719143]

47. Guo H; Fu H; Jin L; Huang S; Li X, Quantification of synergistic, additive and antagonistic effects of aerosol components on total oxidative potential. Chemosphere 2020, 252, 126573.

48. Luo H; Zeng Z; Zeng G; Zhang C; Xiao R; Huang D; Lai C; Cheng M; Wang W; Xiong W; Yang Y; Qin L; Zhou C; Wang H; Zhou Y; Tian S, Recent progress on metal-organic frameworks based- and derived-photocatalysts for water splitting. Chemical Engineering Journal 2020, 383, 123196.

49. Huang C; Zhang C; Huang D; Wang D; Tian S; Wang R; Yang Y; Wang W; Qin F, Influence of surface functionalities of pyrogenic carbonaceous materials on the generation of reactive species towards organic contaminants: A review. Chemical Engineering Journal 2021, 404, 127066.

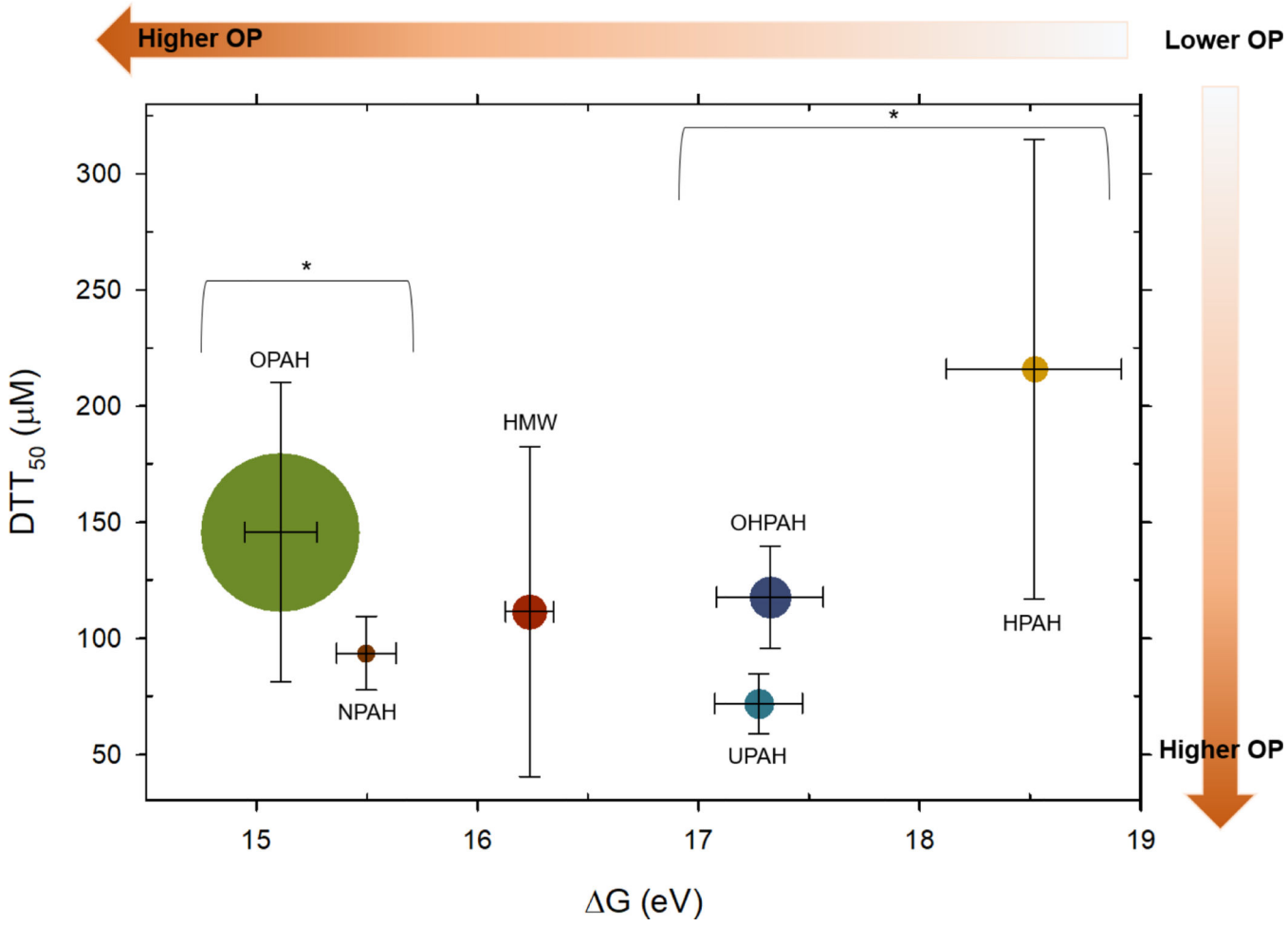

Figure 1.

Graph showing the average PAH class DTT_{50} concentration (μM) as a function of the average PAH class reduction potential (ΔG) of PAHs measured in this study. The size of each data point represents the proportional percent composition of each class of PAHs measured in 96 ambient $PM_{2.5}$ collected in Northwest Washington State (USA) (2016–2018) [23]. Vertical crosshairs represent one standard error for DTT_{50} (μM), and horizontal crosshairs represent one standard error of the average PAH class reduction potential (ΔG). Applying the Dunn Method to the Kruska-Wallis One-way ANOVA on ranks test (due to different number of compounds in each class), OPAH and NPAH ΔG values (eV) were significantly different (p-value ≤ 0.05) from the UPAH, OHPAH, and HPAH classes of PAHs, indicated with *. Using the same statistical test there were no significant differences between the average DTT_{50} of any of the PAH classes.

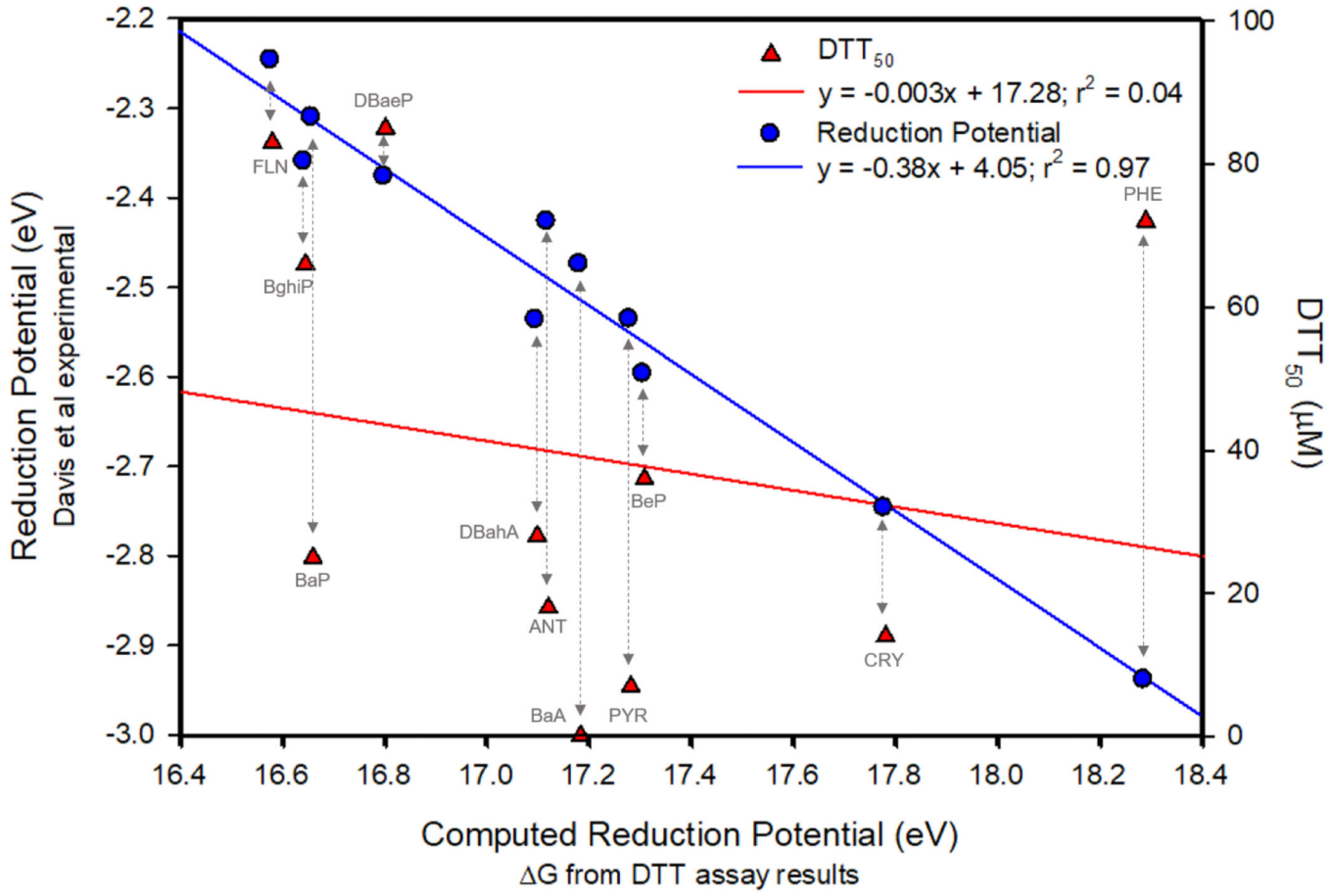

Figure 2.

Comparison plot showing on x-axis the computed ΔG (eV) values for listed PAHs compared to available experimental literature reduction potential values (blue), and DTT_{50} concentrations (red). Blue circles indicate linear relation ($r^2 = 0.97$) between experimental reduction potential[49] of indicated PAHs with the computed reduction potential calculated from the DTT assay results (ΔG eV). Red triangles indicate the DTT_{50} concentration (μM) compared to the calculated reduction potential are not linearly related ($r^2 = 0.04$).

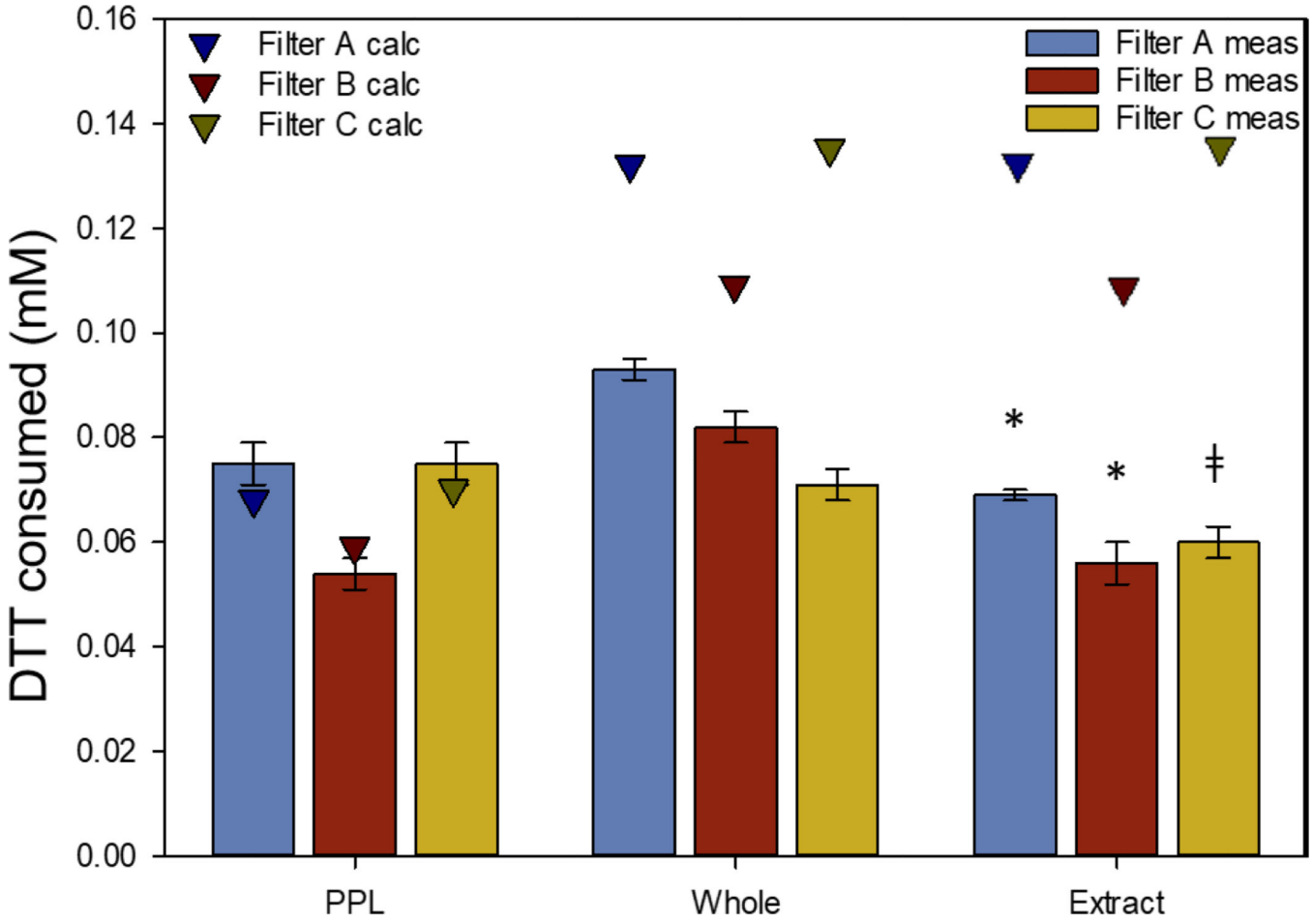

Figure 3.

DTT consumption assay results for PAH mixtures. Bars represent the DTT consumption for PPL mixtures, whole PAH mixtures, and filter extracts. Mixtures were prepared to match measured PAH concentrations in ambient $PM_{2.5}$ filters A, B and C (± SE). The * indicates that Extract measurements were significantly (p-value ≤ 0.05) different from the whole mixture measurements for 2 of the filters (Filters A and B). The ǂ indicates that the extract measurement for Filter C was significantly different than the PPL mixture. Triangles represent predicted DTT consumption using the linear relationships of PAHs measured in the filter extracts, assuming an additive mixture effect.

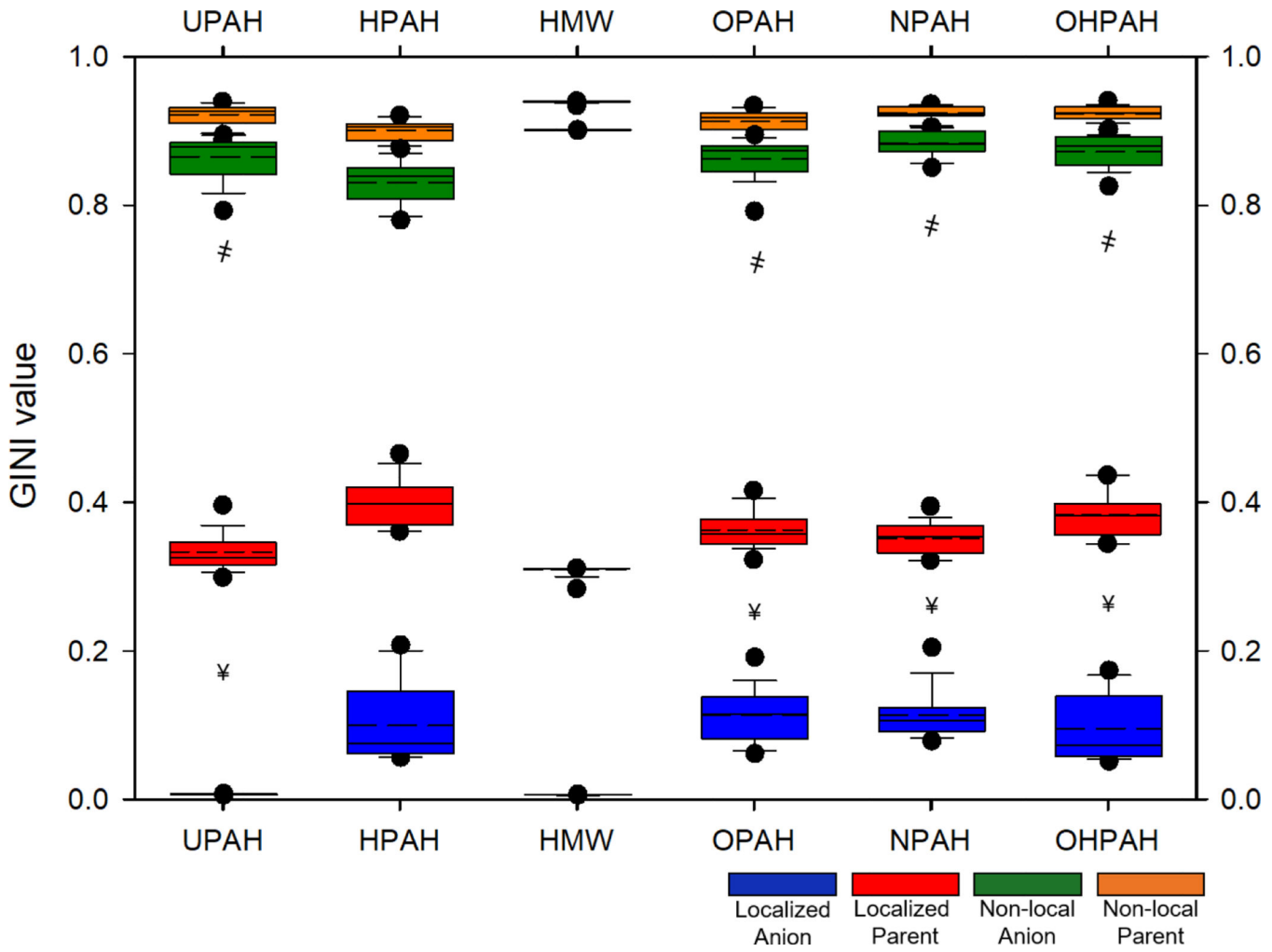

Figure 4.

Box and whisker plots showing the GINI values per class of PAH as computed in four different scenarios. Red (parent) and blue (radical anion) boxes show inter-quartile GINI values for localized electrons only, and orange (parent) and green (radical anion) boxes show the inter-quartile values for localized and delocalized electrons. Whiskers represent the standard deviation of the data in each class, dots show the 5^{th} and 95^{th} percentiles. The solid line in each bar represents the median of the data, while the dotted line is the mean value. * indicates a statistically significant difference (p-value ≤ 0.05) between the parent and radical anionic GINI value for localize electrons only. ≠ indicates a statistically significant difference (p-value ≤ 0.05) between the parent and radical anion GINI values for both localized and delocalized electrons as determined using the Kruskal-Wallis One-way ANOVA on ranks.

Table 1.

Statistically significant (p-value < 0.05) correlation results between PAH molecular mass (AMU), concentration required to use 50% of the DTT in the assay (DTT_{50}), the ΔG_{rxn} of the reduction of the PAH (eV), the difference in GINI value for localized electrons (Parent – Anion), the difference in GINI value for delocalized electrons (Parent – Anion), type and number of substituents, and structural components. “All” indicates correlations between parameter and the entire suite of 135 PAHs measured in the assay. Subclasses of PAHs are identified by letters as follows: “U” (UPAHs), “N” (NPAHs), “O” (OPAHs), “H” (HPAHs), “W” (HMW PAHs), and “OH” (OHPAHs). Grayed in boxes represent the X:X in the correlation matrix.

	Molecular Mass (AMU)	**DTT_{50} (μM)**	**ΔG_{rxn} (eV)**	**(P-A) GINI localized e^-**	**(P-A) GINI delocalized e^-**	**Substituent**	**Structural Component**
Molecular Mass (AMU)		All	All, U, N, OH	All, U, O, OH, N, H	U, H, N, OH	All	U, N, OH
DTT_{50} (μM)	All						OH
ΔG_{rxn} (eV)	All, U, N, OH			All, U, N, OH	All, U, N, OH	All, N	U, O
(P-A) GINI localized e^-	All, U, O, OH, N, H		All, U, N, OH		All, U, H, W, N, OH	All, H, N, O, OH	All, U, W, OH
(P-A) GINI delocalized e^-	U, H, N, OH		All, U, N, OH	All, U, H, W, N, OH		All, N	U, H, OH
Substituent	All		All, N	All, H, N, O, OH	All, N		
Structural Component	U, N, OH	OH	U, O	All, U, W, OH	All, U, W, OH		